Supporting Information

Electronic Metal-Support Interaction Constructed for Preparing Sinter-Resistant Nano-Platinum Catalyst with Redox Property

*Bin Zheng, *[a,b] Jialong Duan, [a] and Qunwei Tang *[a]*

[a] Institute of New Energy Technology, College of Information Science and Technology, Jinan University, Guangzhou, 510632, P. R. China.

[b] School of Chemistry and Chemical Engineering, Liaocheng University, Liaocheng, 252000, P. R. China.

[*] Corresponding author.

E-mail addresses: zhengbin@jnu.edu.cn (B. Zheng)

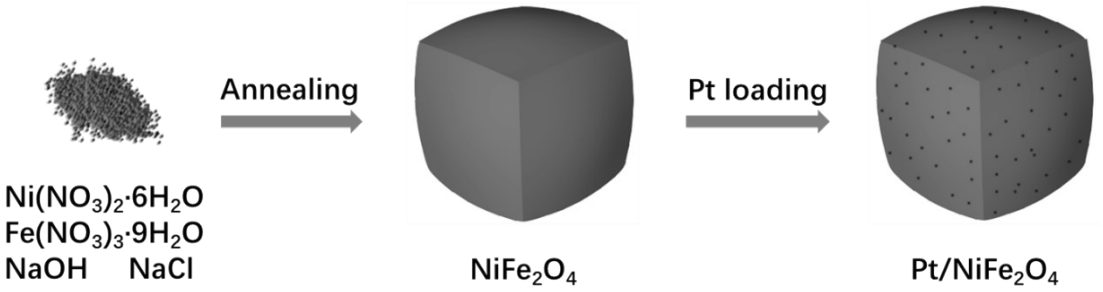

Scheme S1. Schematic illustration of the preparation of $NiFe_2O_4$ and $Pt/NiFe_2O_4$ samples.

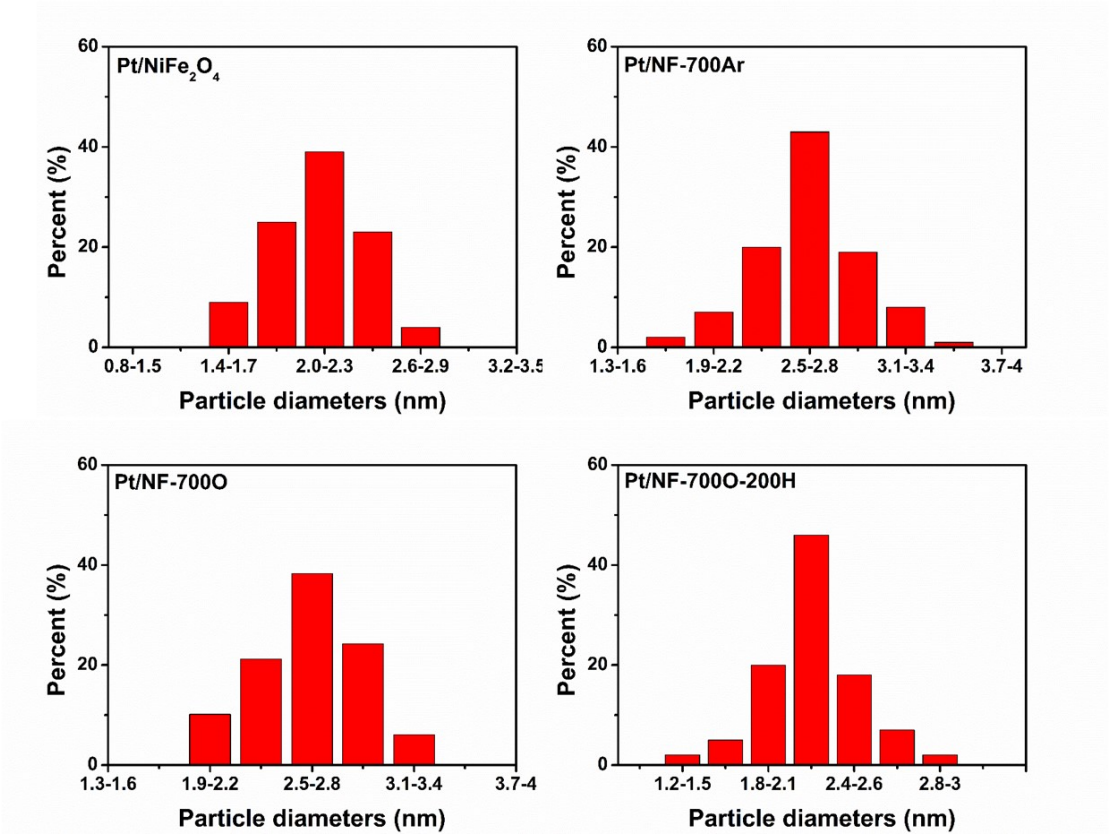

Fig. S1 Pt NPs size distributions of $Pt/NiFe_2O_4$, Pt/NF-700Ar, Pt/NF-700O and Pt/NF-700O-200H samples.

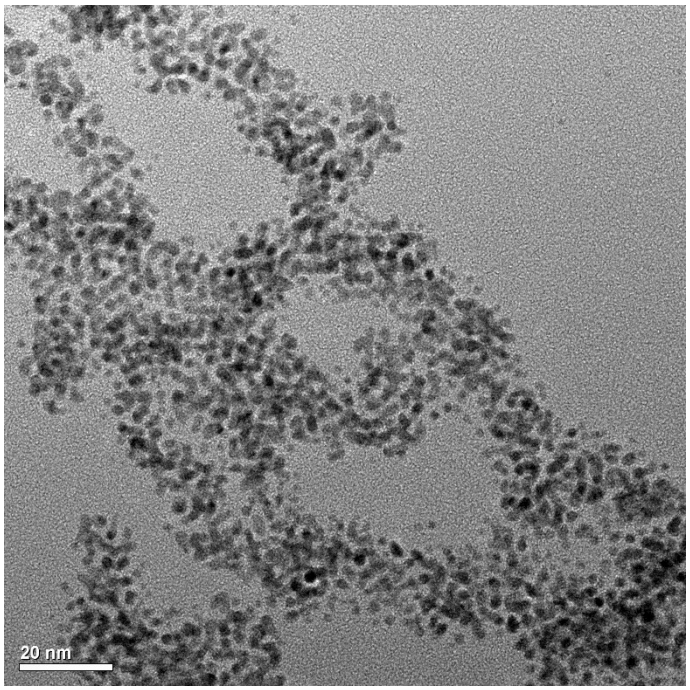

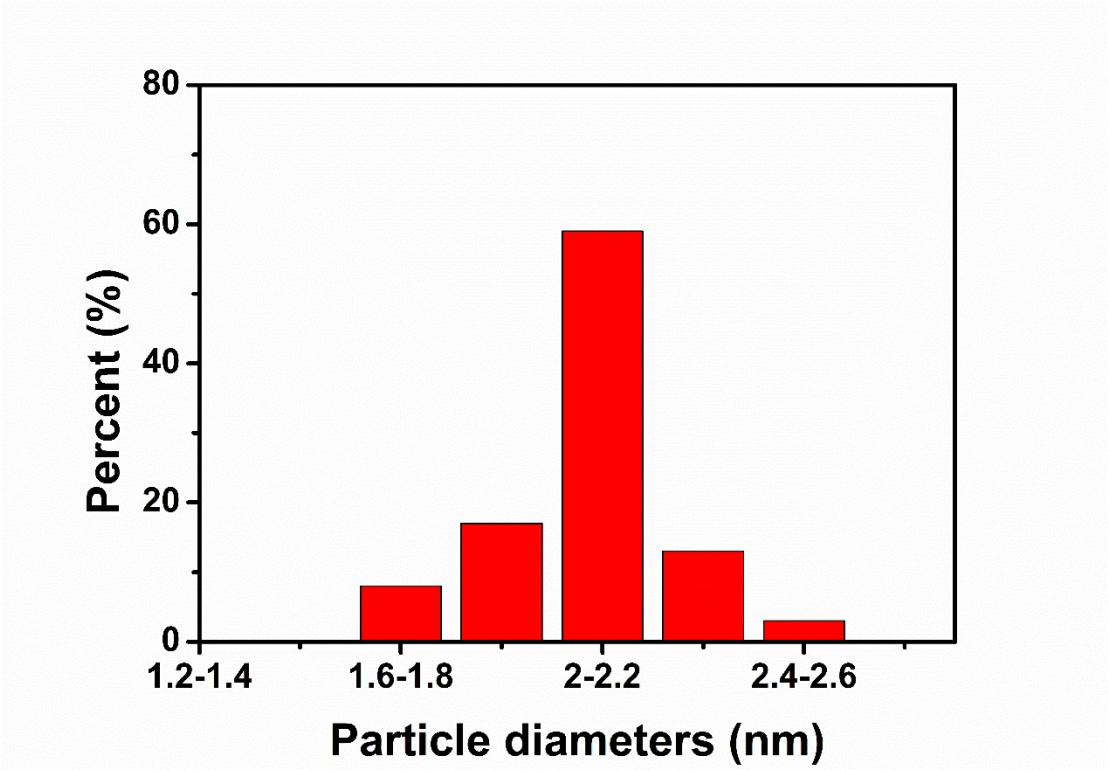

Fig. S2 TEM image and Pt NPs size distributions of Pt colloids.

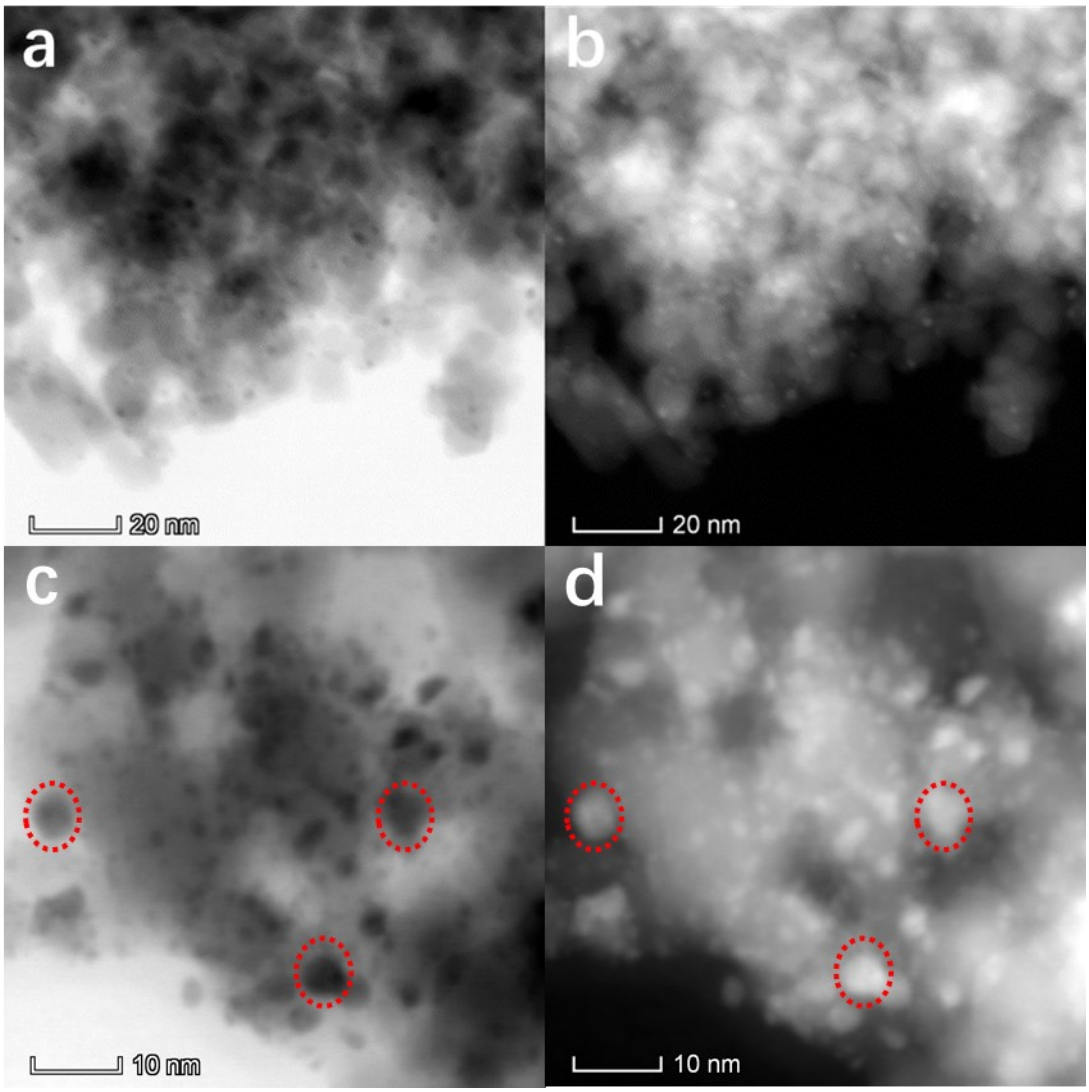

Fig. S3 STEM images of Pt/α-Fe_2O_3 (a, b) and Pt/Fe-700O (c, d) samples.

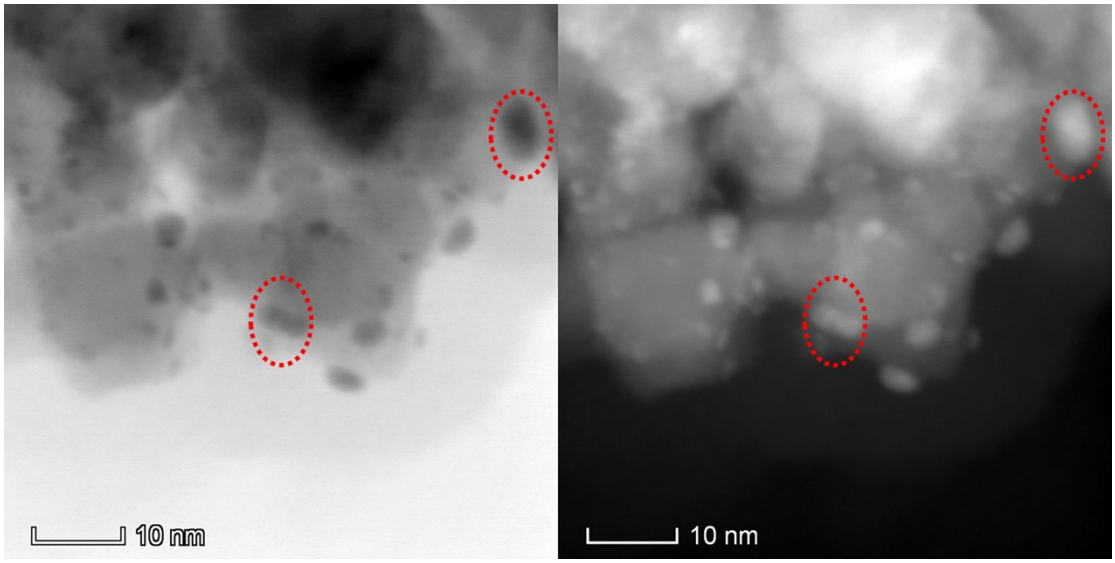

Fig. S4 STEM images of Pt/Fe-700O after H_2 reduction.

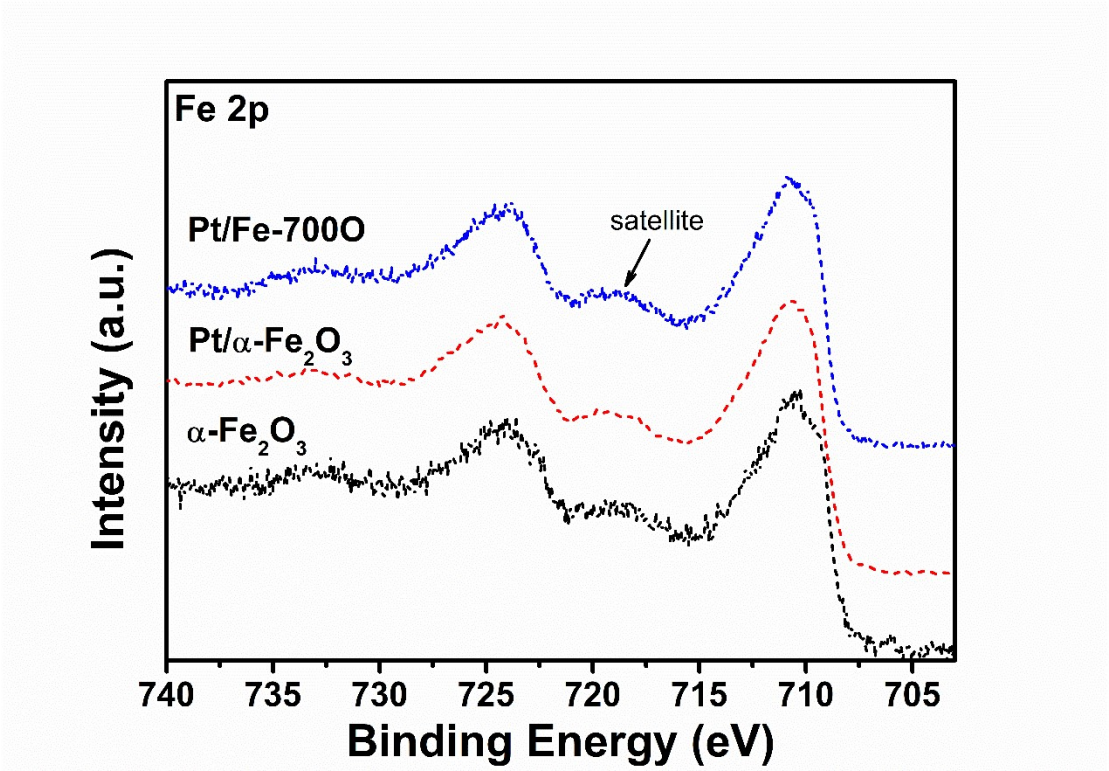

Fig. S5 Fe 2p XPS spectra of α-Fe_2O_3 support, Pt/α-Fe_2O_3 and Pt/Fe-700O samples. C 1s at 284.6 eV is taken as reference.

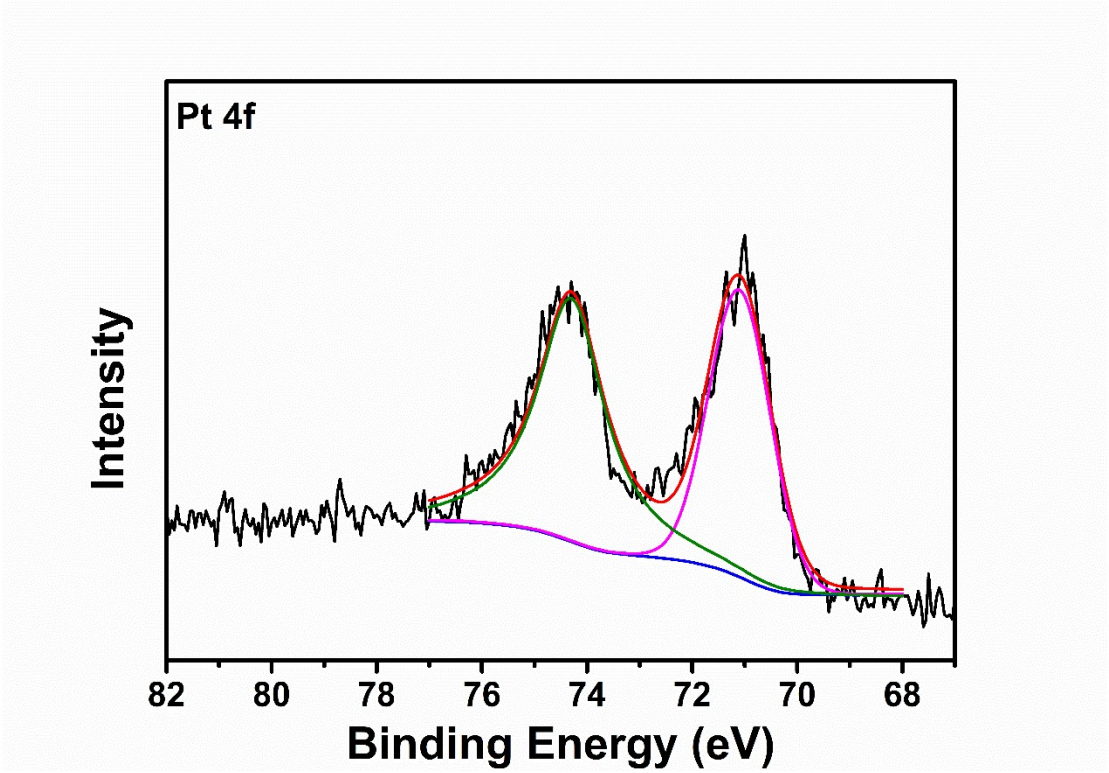

Fig. S6 Pt 4f XPS spectrum of Pt colloid nanoparticles. C 1s at 284.6 eV is taken as reference.

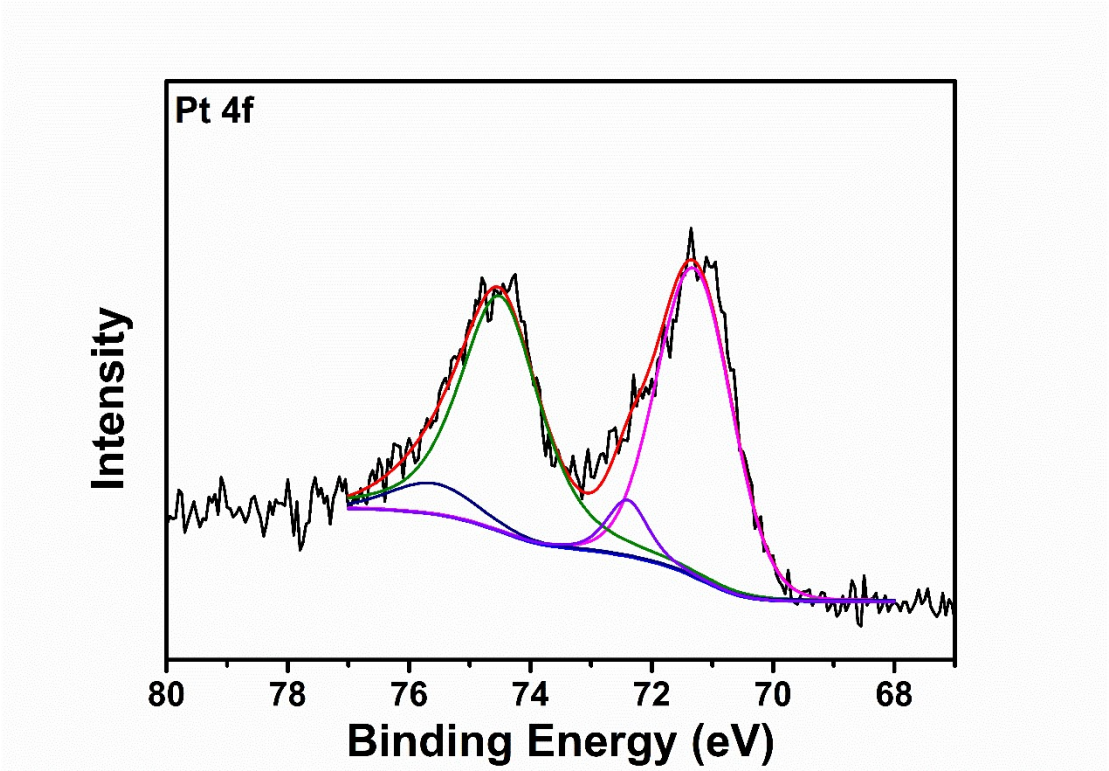

Fig. S7 Pt 4f XPS spectrum of Pt/α-Fe_2O_3. C 1s at 284.6 eV is taken as reference.

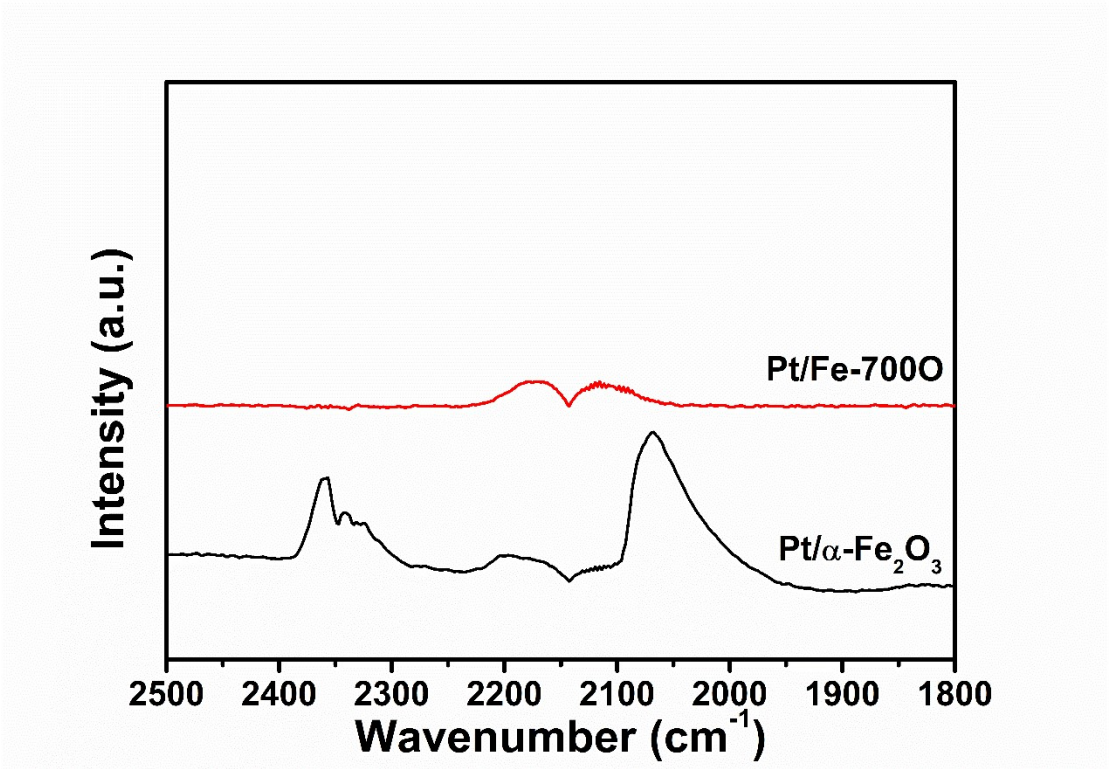

Fig. S8 In-situ DRIFT CO adsorption spectra of Pt/α-Fe_2O_3 and Pt/α-Fe_2O_3-700O (Pt/Fe-700O) samples.

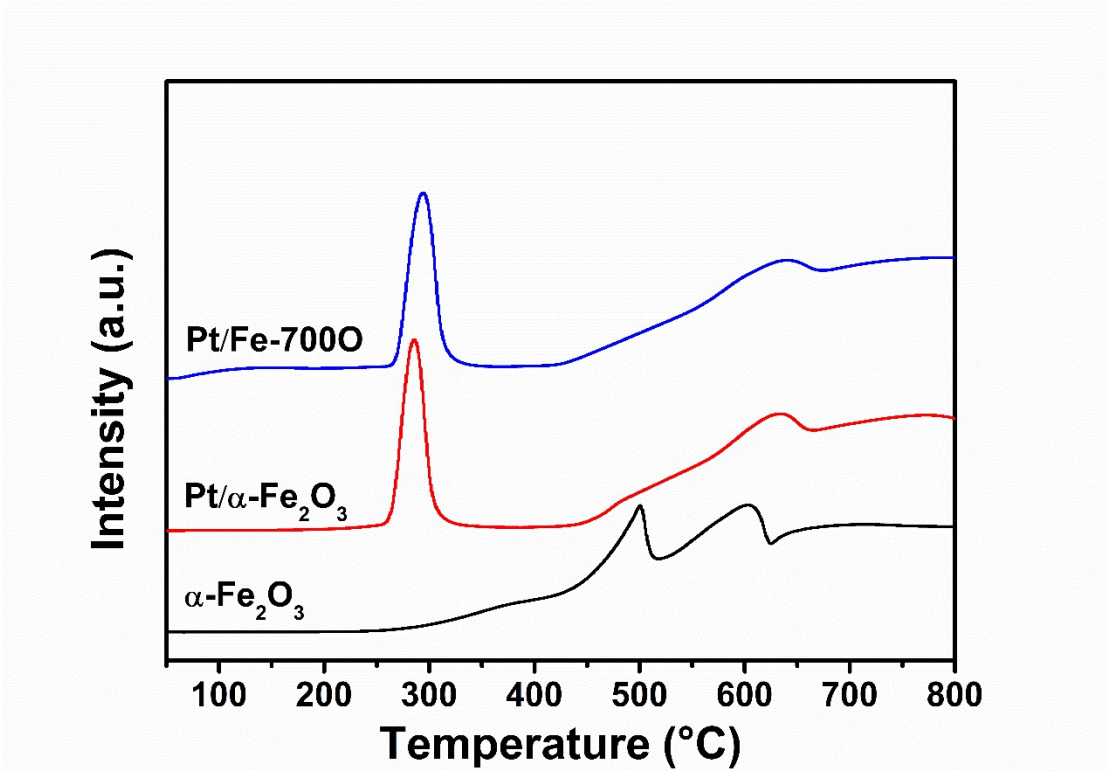

Fig. S9 H_2-TPR profiles of α-Fe_2O_3, Pt/α-Fe_2O_3 and Pt/Fe-700O samples.

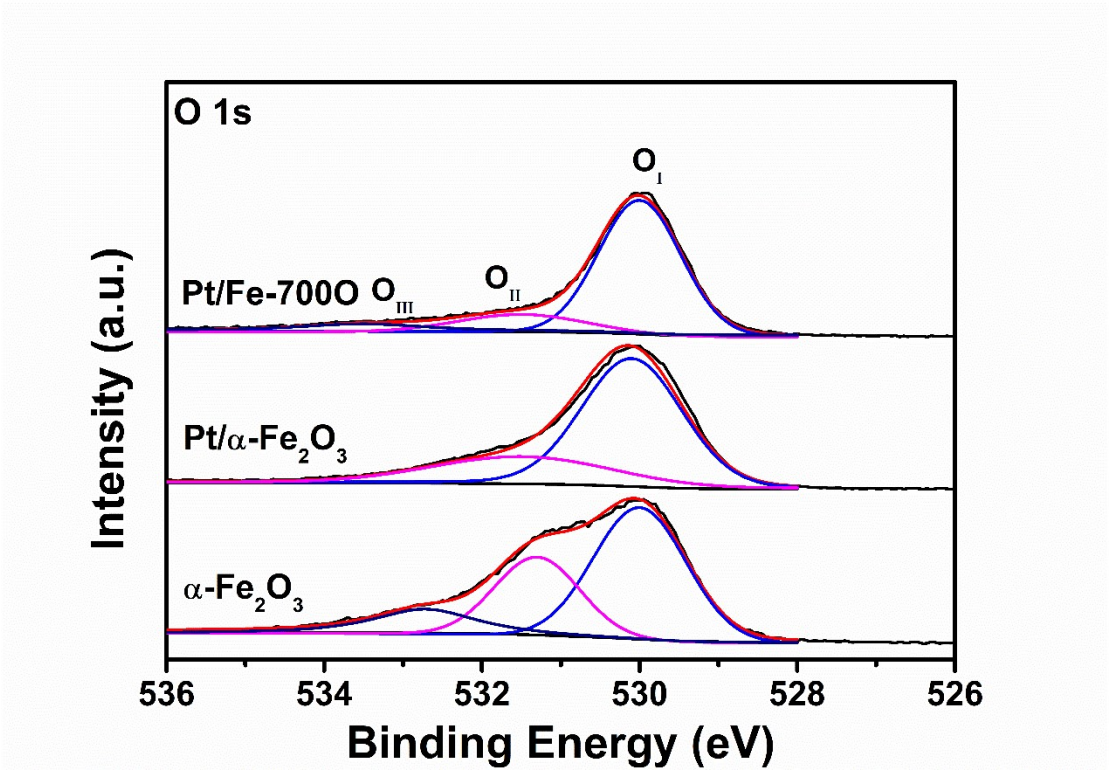

Fig. S10 O 1s XPS spectra of α-Fe_2O_3 support, Pt/α-Fe_2O_3 and Pt/Fe-700O samples.

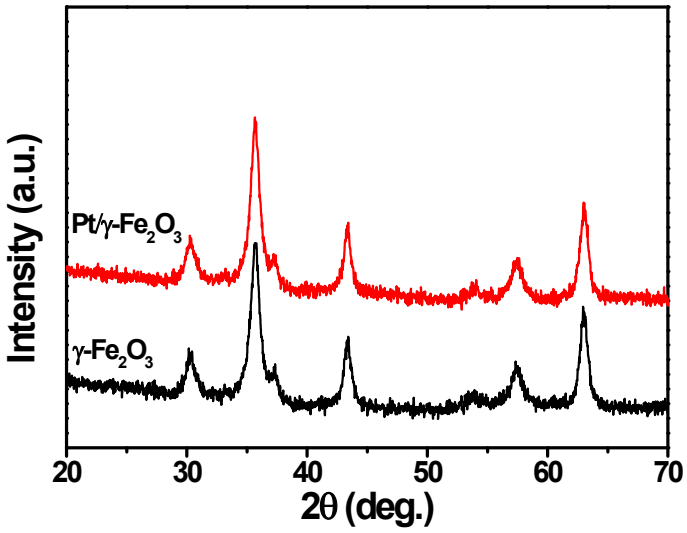

Fig. S11 XRD patterns of prepared γ-Fe_2O_3 and Pt/γ-Fe_2O_3 samples.

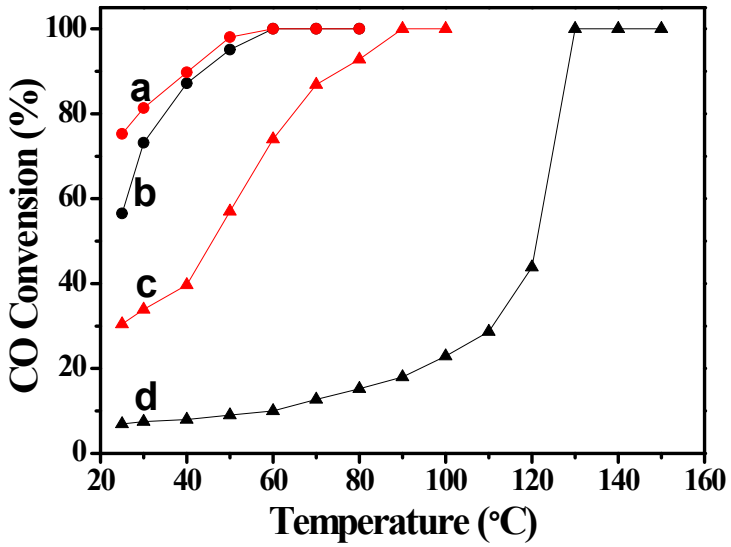

Fig. S12 CO oxidation activities of a) Pt/γ-Fe_2O_3, b) Pt/α-Fe_2O_3 under moisture condition and c) Pt/γ-Fe_2O_3, d) Pt/α-Fe_2O_3 under dry condition. Reaction conditions: 1 vol% CO, 5 vol% O_2/Ar, (1.8 vol% H_2O) and Ar balance, GHSV: 60000 $mL \cdot g^{-1} \cdot h^{-1}$.

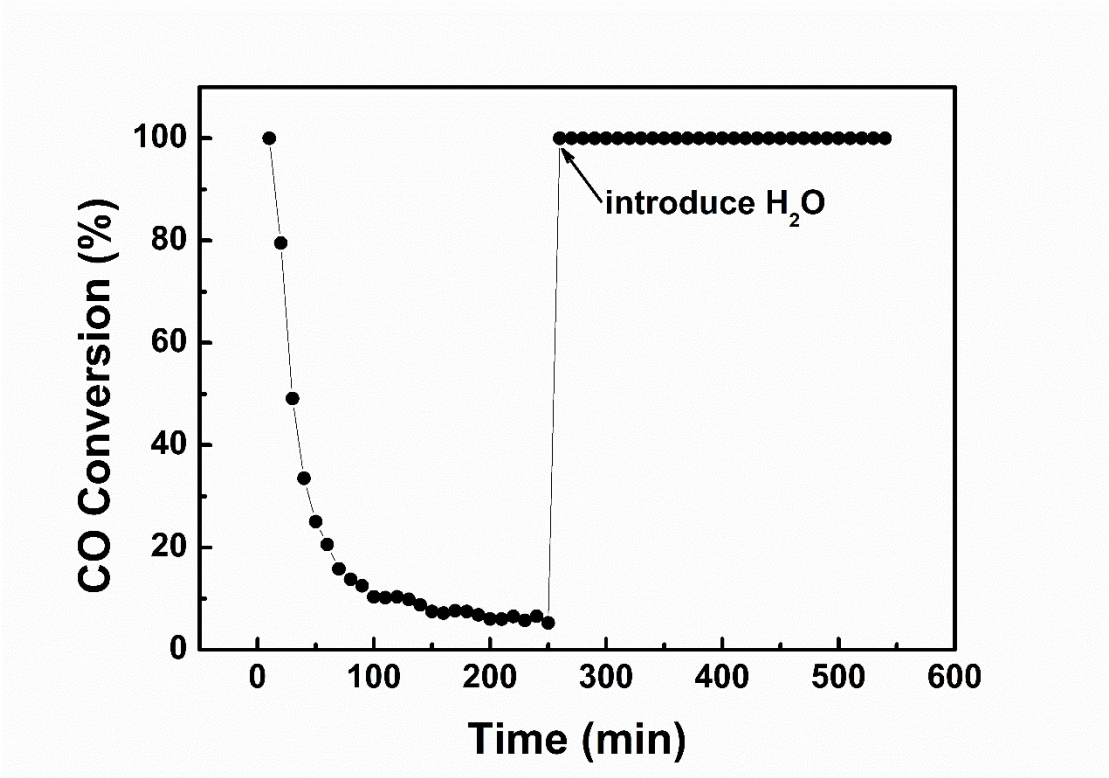

Fig. S13 CO conversion versus time on stream over $Pt/NiFe_2O_4$ in the absence and presence of water vapor.

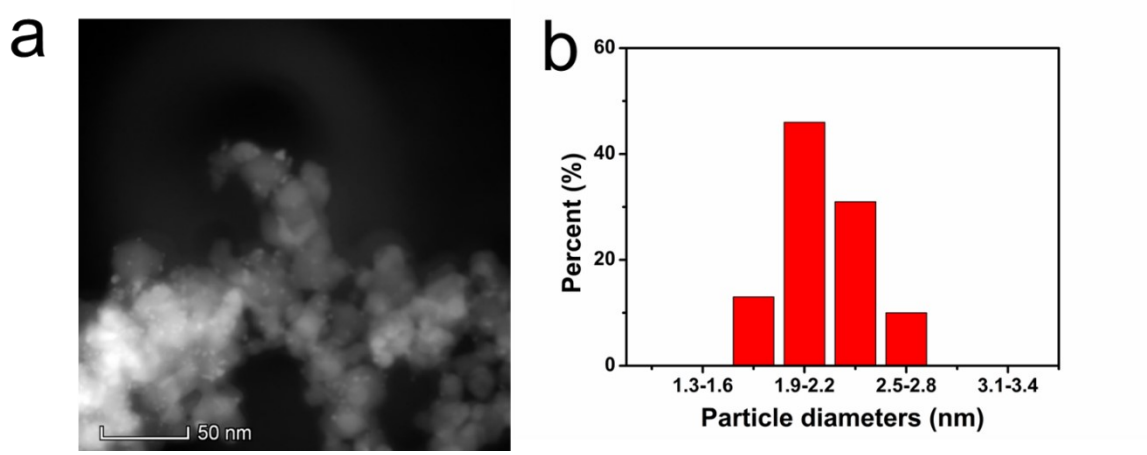

Fig. S14 HAADF-STEM image (a) and Pt NPs size distributions (b) of Pt/$NiFe_2O_4$ catalyst after storage and long-period CO catalytic oxidation process.

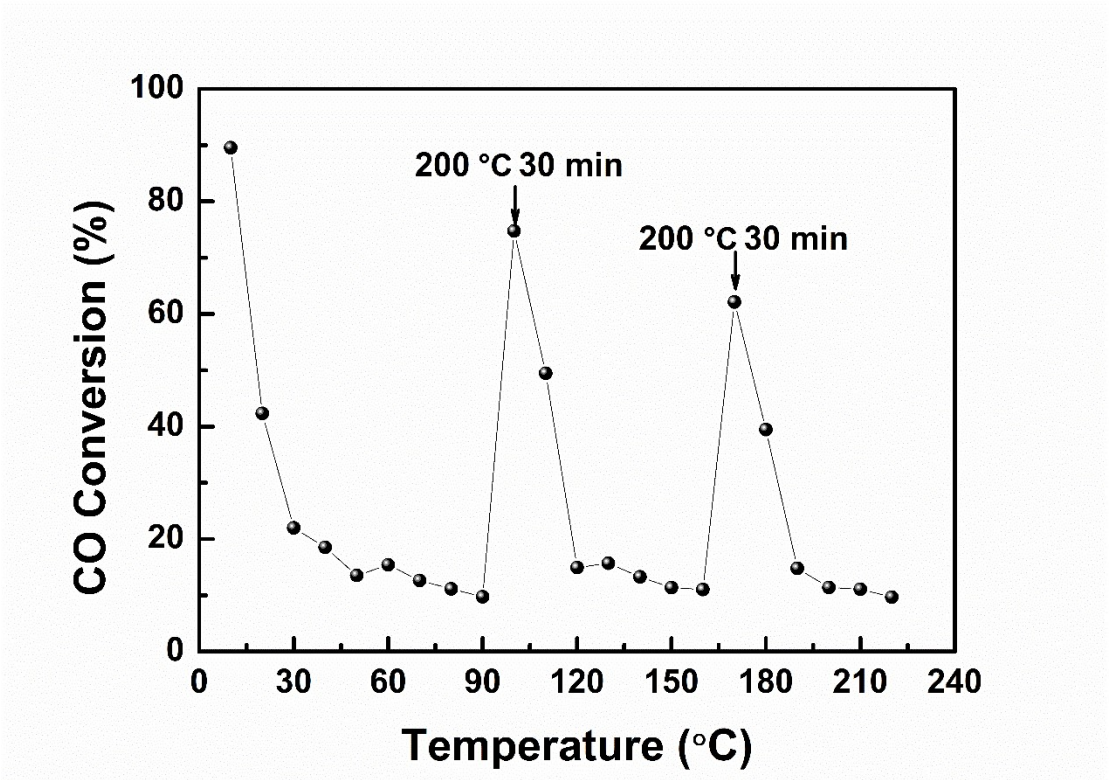

Fig. S15 Catalytic performance of supported-Pt catalysts in CO oxidation as a function of reaction time at room temperature.

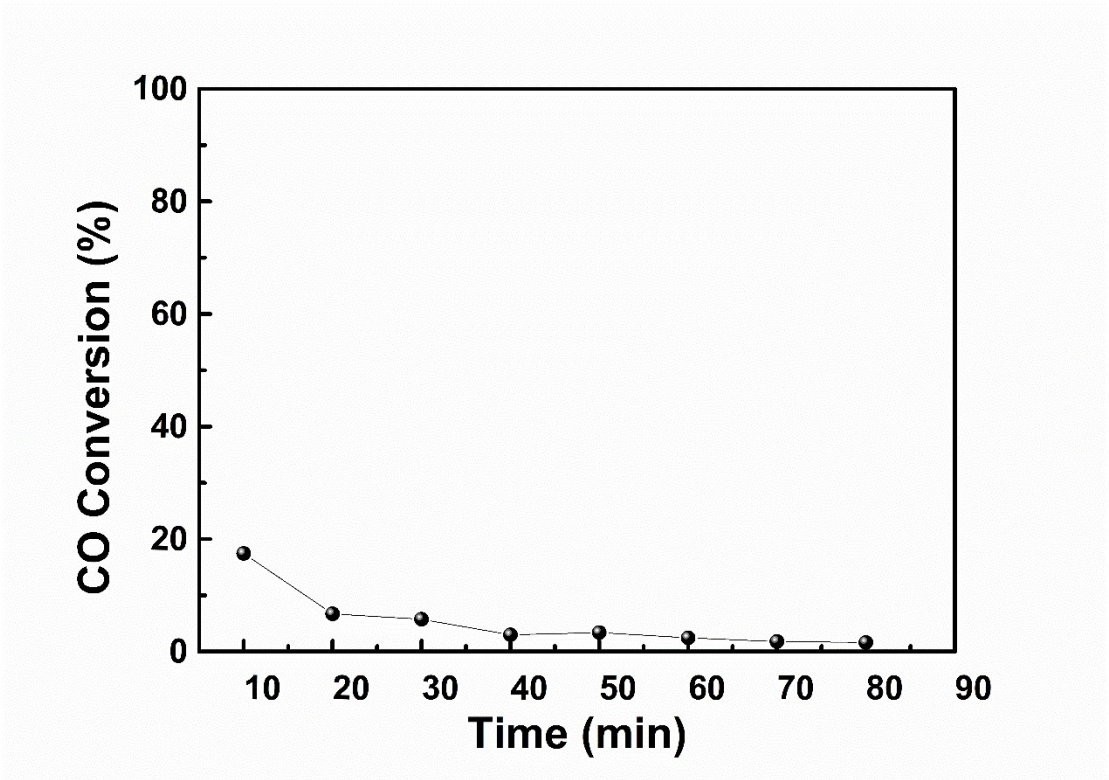

Fig. S16 CO conversion versus time on stream over $Pt/NiFe_2O_4$ under moisture atmosphere without O_2.

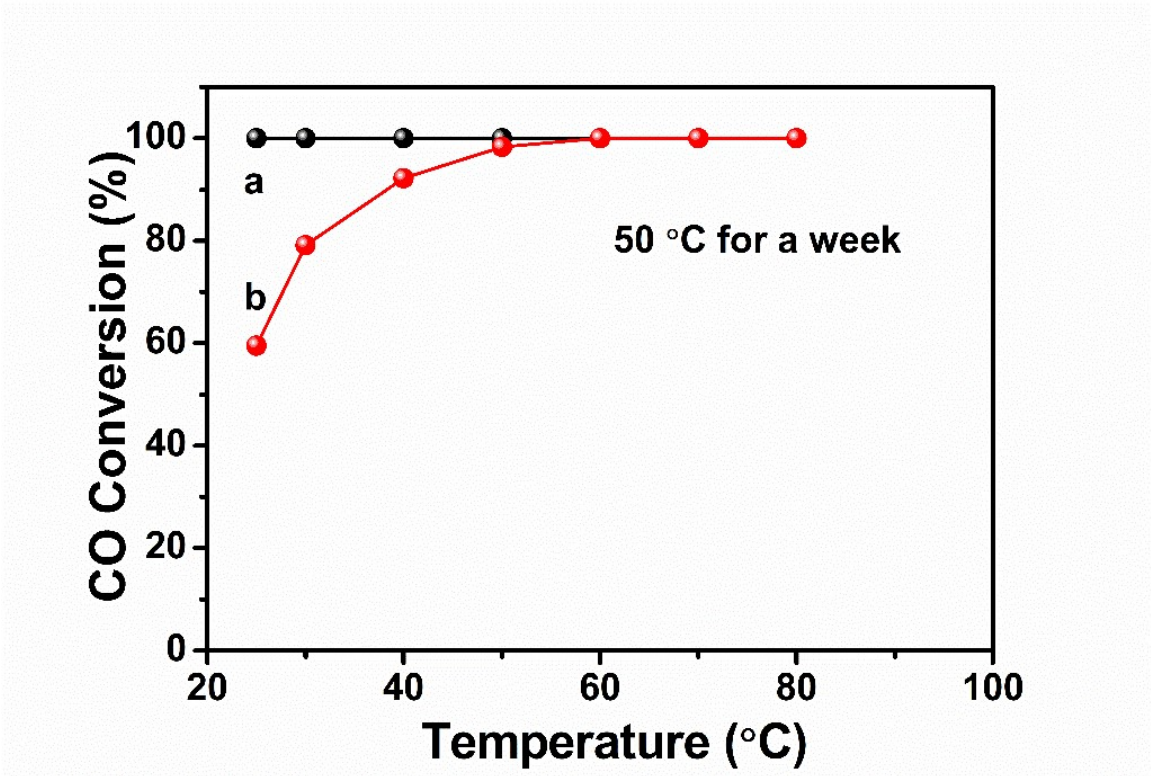

Fig. S17 Catalytic CO oxidation activities of a) Pt/$NiFe_2O_4$, b) Pt/ferrihydrite after treated at 50 ℃ for a week. Reaction conditions: 1 vol% CO, 5 vol% O_2/Ar, 1.8 vol% H_2O and Ar balance, GHSV: 60000 $mL \cdot g^{-1} \cdot h^{-1}$.

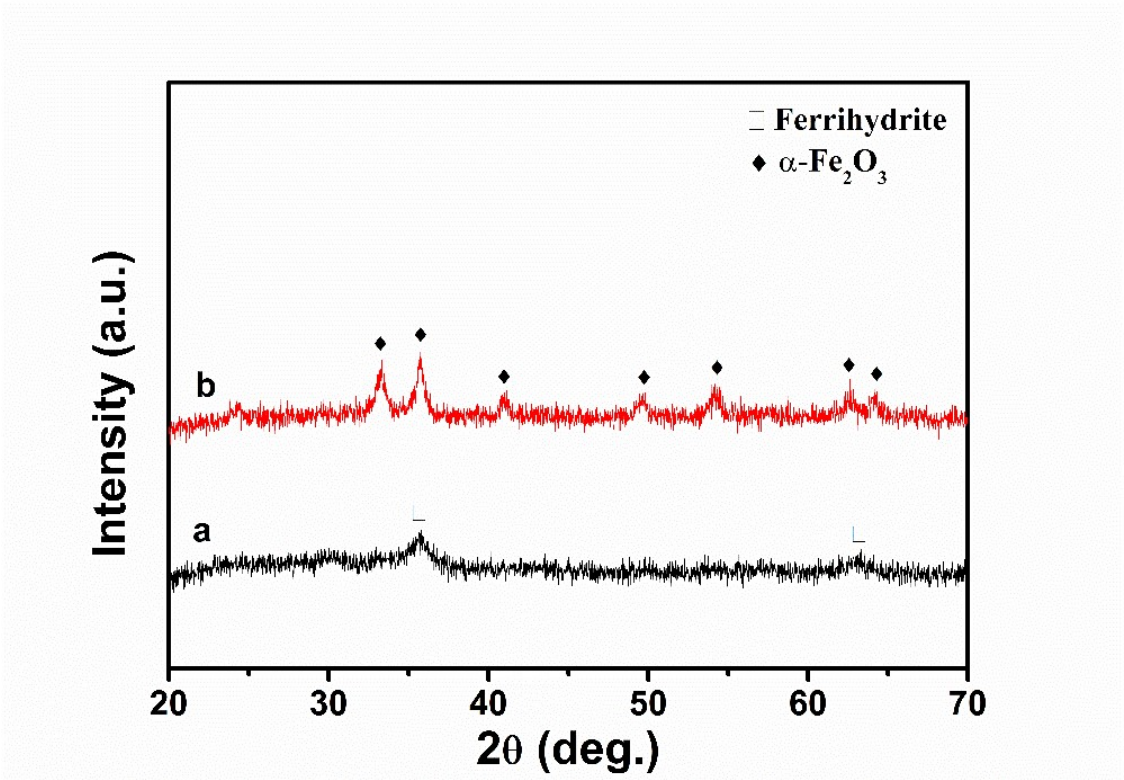

Fig. S18 XRD patterns of Pt/ferrihydrite (a) and Pt/ferrihydrite after 50 ℃ treatment for a week (b).

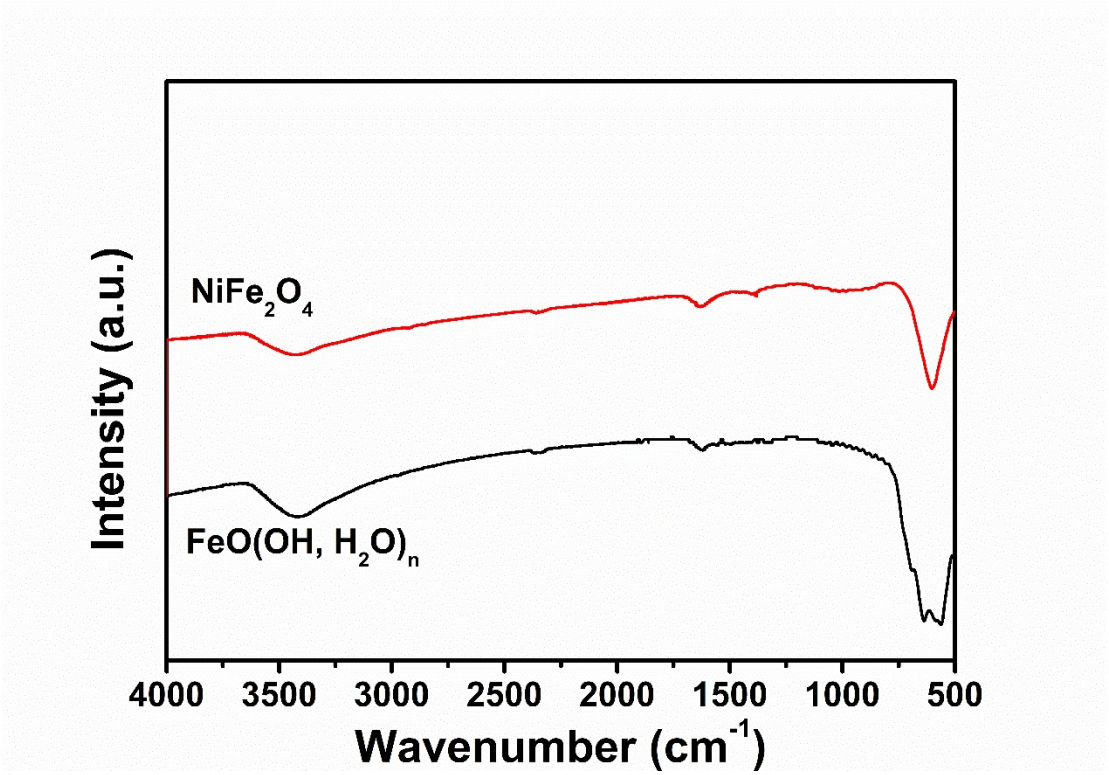

Fig. S19 FT-IR spectra of $FeO(OH, H_2O)_n$ and $NiFe_2O_4$ samples.

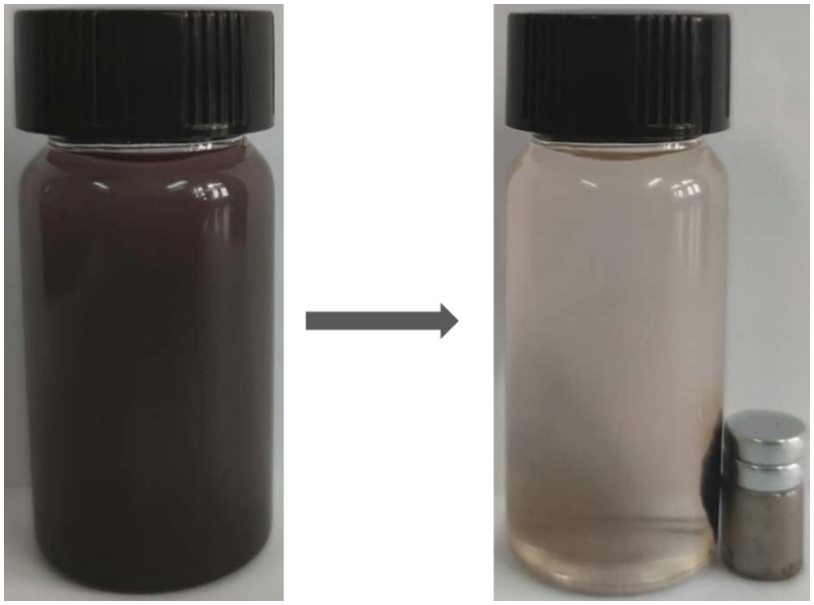

Fig. S20 The magnetic properties of $Pt/NiFe_2O_4$ sample.

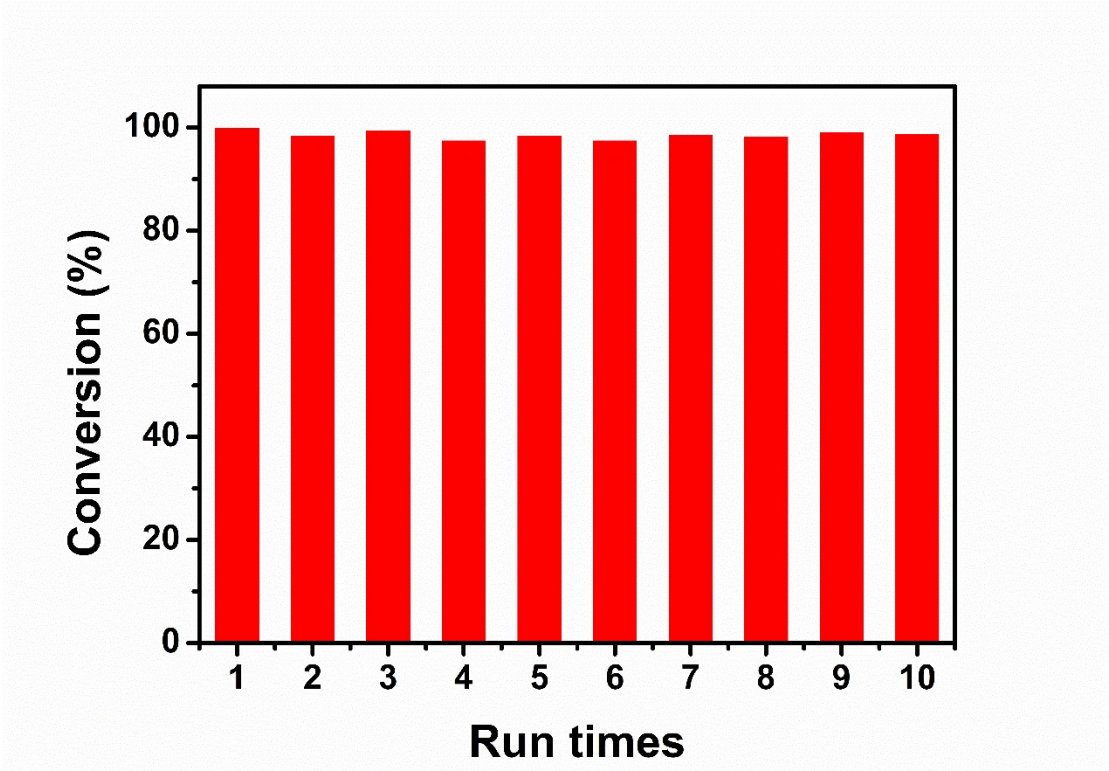

Fig. S21 Recycling tests over the $Pt/NiFe_2O_4$ catalyst. Reaction conditions: t = 25 °C, P = 5 bar, m_{cat} = 50 mg, 1 mmol nitrobenzene, 15 mL of toluene as solvent, reaction time: 2h.

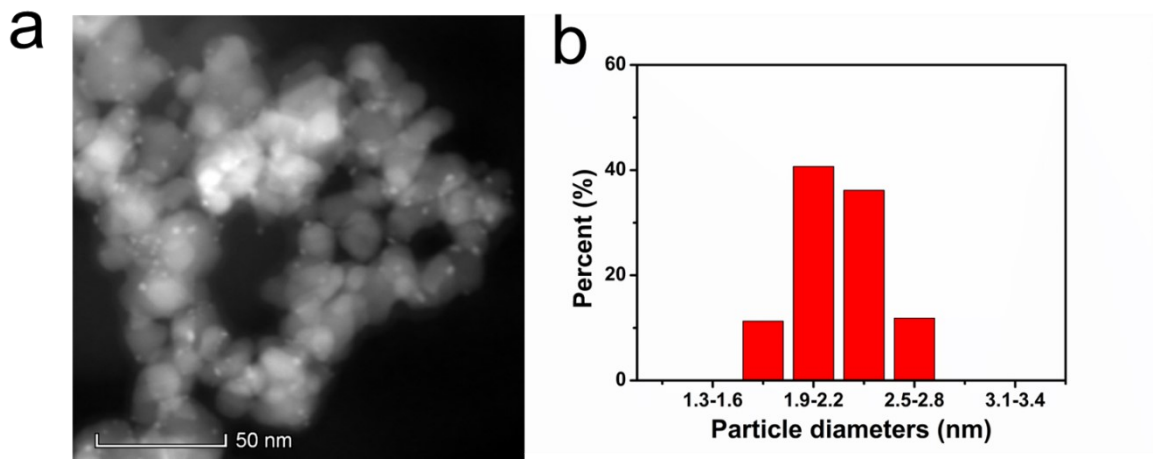

Fig. S22 HAADF-STEM image (a) and Pt NPs size distributions (b) of Pt/$NiFe_2O_4$ catalyst after ten recycling tests for hydrogenation of nitrobenzene.

Table S1. Texture properties of $NiFe_2O_4$ and $Pt/NiFe_2O_4$ samples treated at different conditions.

Samples	S_{BET} ($m^2 \cdot g^{-1}$)	Pore Volume ($cm^3 \cdot g^{-1}$)	Pore Size [a] (nm)
$NiFe_2O_4$	34.8	0.10	119.8
$Pt/NiFe_2O_4$	36.9	0.08	94.9
Pt/NF-700Ar	22.7	0.03	85.6
Pt/NF-700O	17.9	0.03	84.7
Pt/NF-700O-200H	31.3	0.06	82.2

[a] Average pore size calculated from desorption branches using BJH model.

Table S2. Texture properties of α-Fe_2O_3 and Pt/α-Fe_2O_3 samples treated at different conditions.

Samples	S_{BET} ($m^2 \cdot g^{-1}$)	Pore Volume ($cm^3 \cdot g^{-1}$)	Pore Size [a] (nm)
α-Fe_2O_3	33.2	0.18	138.8
Pt/α-Fe_2O_3	31.2	0.17	135.6
Pt/Fe-700O	16.5	0.10	92.2

[a] Average pore size calculated from desorption branches using BJH model.

Table S3. The surface element amounts of $NiFe_2O_4$ and $Pt/NiFe_2O_4$ samples treated at different conditions.

Samples	Na	O	Ni	Fe	Pt	Fe_t^{3+}/Fe_o^{3+}	O_{II}/O_I
$NiFe_2O_4$	5.43	58.64	11.52	24.41		1.14	0.75
$Pt/NiFe_2O_4$-F	4.79	57.69	12.55	23.80	1.17	1.10	0.78
$Pt/NiFe_2O_4$	4.68	58.72	11.46	23.41	1.73	1.16	0.81
Pt/NF-700Ar	4.84	60.57	11.86	21.01	1.71	1.13	0.79
Pt/NF-700O	4.79	59.73	12.02	21.80	1.67	1.11	0.76
Pt/NF-700O-200H	2.66	56.56	12.57	26.63	1.58	1.14	0.80

Table S4. H_2 consumption of supported Pt catalyst calculated from H_2-TPR profiles.

Samples	H_2 consumption of the first peak ($mmol \cdot g^{-1}$)	H_2 consumption of the second peak ($mmol \cdot g^{-1}$)	H_2 consumption of the third peak ($mmol \cdot g^{-1}$)
$Pt/NiFe_2O_4$	1.37	0.19	6.64
Pt/NF-700Ar	0.51	1.82	6.10
Pt/NF-700O	0	2.32	7.38
Pt/NF-700O-200H	0.42	1.75	6.08